



Open Archive TOULOUSE Archive Ouverte (OATAO)

OATAO is an open access repository that collects the work of Toulouse researchers and makes it freely available over the web where possible.

This is an author-deposited version published in : <http://oatao.univ-toulouse.fr/>
Eprints ID : 3223

To link to this article : DOI:[10.1016/j.electacta.2009.08.052](https://doi.org/10.1016/j.electacta.2009.08.052)
URL : <http://dx.doi.org/10.1016/j.electacta.2009.08.052>

To cite this version :

Gibilaro, M. and Massot, Laurent and Chamelot, Pierre and Cassayre, Laurent and Taxil , Pierre (2009) *Electrochemical extraction of europium from molten fluoride media*. Electrochimica Acta, vol. 55 (n° 1). pp. 281-287. ISSN 0013-4686

Electrochemical extraction of europium from molten fluoride media

M. Gibilaro^{a,b}, L. Massot^{a,b,*}, P. Chamelot^{a,b}, L. Cassayre^{a,b}, P. Taxil^{a,b}

^a Université de Toulouse, INPT, UPS, Laboratoire de Génie Chimique, Département Procédés Electrochimiques, F-31062 Toulouse cedex 09, France

^b CNRS, Laboratoire de Génie Chimique, F-31062 Toulouse cedex 09, France

A B S T R A C T

This work concerns the extraction of europium from molten fluoride media. Two electrochemical ways have been examined: (i) the use of a reactive cathode made of copper and (ii) the co-deposition with aluminium on inert electrode, leading to the formation of europium–copper and europium–aluminium alloys, respectively, as identified by SEM-EDS analysis. Cyclic voltammetry and square wave voltammetry were used to identify the reduction pathway and to characterise the step of Cu–Eu and Al–Eu alloys formation. Then, electrochemical extractions using the two methodologies have been performed with extraction efficiency around 92% for copper electrode and 99.7% for co-reduction with aluminium ions.

Keywords:

Molten fluorides

Europium

Reactive electrode

Electrochemical extraction

Co-reduction

1. Introduction

In France, alternative solutions for radioactive wastes management are under examination since 1991, in the frame of Partitioning and Transmutation (P&T) concepts aiming at significantly reducing the amount of radiotoxic nuclear waste at the end of the fuel cycle [1]. In these concepts, the most radiotoxic elements (Pu, Am, Cm) are to be burned by transmutation and for this purpose an efficient separation of actinides (An) from lanthanides (Ln) is required. The present hydrometallurgical PUREX process allows extraction of uranium and plutonium for further reuse in MOX fuels. But, concerning the new types of fuels for future generation reactors (i.e. metallic, nitride, carbide, CER-MET) of fuels with inert matrices, a complete recovery of all An is desired, and aqueous media have not yet proven to be the adequate solvents to dissolve the fuels. Another route could consist of using pyrochemical processes involving molten salts, which are currently studied as alternative media due to their good physico-chemical properties (as solvation for example), but also for some advantages as a faster reprocessing with much shorter cooling times of the fuel, compactness of the reprocessing process yielding the possibility of direct connection of the reprocessing unit with the reactor, etc. Recent progresses have been realised for An extraction in molten salts using extractive reduction [2] and electrorefining [3]. After

An extraction, Ln have to be completely removed from the salt in order to recycle the molten solvent. On top of these P&T concepts, the Molten Salt Reactor, which is one of the six nuclear reactors concept evaluated in the frame of the Generation IV Forum, requires an online processing of the fuel in order to remove fission products and particularly Ln which have a poisonous effect on the nuclear reactions taking place in the core of the reactor [4].

Our laboratory is highly interested in Ln extraction from fluoride solvent and has already succeeded in the extraction of several lanthanides in LiF–CaF₂ [5]. This article is focused on the europium extraction from this medium containing EuF₃. In a recent study, we have demonstrated that Eu(III) is reduced in two steps in the LiF–CaF₂ eutectic on a Mo inert electrode at 840 °C according to [6]:



The main issue of this previous work is that the electroreduction of Eu(II) into Eu metal takes place at a more cathodic potential than the solvent ions reduction Li(I). Consequently, the extraction of Eu ions from the molten salt is not conceivable on an inert electrode. An alternative solution may consist of decreasing the electrodeposited metal activity. For this, two different electrochemical processes can be applied: the use of a reactive cathode made of copper [7] or the co-reduction with aluminium ions [8], both yielding Eu-based alloys as cathodic products. In this work, these techniques were used and Cu–Eu or Al–Eu alloys have been characterised by microscopic observation and metallic phase analysis. Finally, the feasibility of Eu(III) extraction has been evaluated

* Corresponding author at: Université de Toulouse, INPT, UPS, Laboratoire de Génie Chimique, Département Procédés Electrochimiques, 118 route de Narbonne, F-31062 Toulouse cedex 09, France. Tel.: +33 5 61 55 81 94; fax: +33 5 61 55 61 39.
E-mail address: massot@chimie.ups-tlse.fr (L. Massot).

with the two different methods and extraction efficiencies have been determined.

2. Experimental

The experimental cell consisted of a vitreous carbon crucible placed in a cylindrical vessel made of refractory steel and closed by a stainless steel lid cooled inside by circulating water. The inner part of the walls was protected against fluoride vapours with a graphite liner containing the experimental crucible. The experiments were performed under an argon gas atmosphere (U-grade: less than 5 ppm O_2), previously dehydrated and deoxygenated using a purification cartridge (Air Liquide). The cell was heated in a programmable furnace and the temperature was measured using a chromel–alumel thermocouple. A more detailed description of the device can be found in previous papers of our group [9].

The electrolytic bath consisted of the eutectic LiF/CaF_2 (SDS Carlo Erba 99.99%) mixture (79/21 molar ratio). Before use, it was dehydrated by heating under vacuum (3×10^{-2} mbar) from room temperature up to its melting point (762 °C) for 72 h. To provide europium and aluminium ions, europium and aluminium trifluoride (SDS Carlo Erba 99.95% and 99.99%, respectively) pellets were introduced into the bath through a lock chamber under argon gas atmosphere.

Electrochemistry: potentiostatic electrolysis mode was used for extractions and elements titration was performed by square wave voltammetry which was proved to be an accurate *in situ* method. For this purpose, an Autolab PGSTAT 30 potentiostat/galvanostat controlled by the research software GPES 4.9 was used.

Characterisation of reduction products: after electrolysis, the cathode surface was examined by scanning electron microscopy (LEO 435 VP) equipped with an energy dispersive spectroscopy (EDS) probe (Oxford INCA 200) for determining the composition of the alloys. Inductively coupled plasma-atomic emission spectroscopy (ICP-AES Jobin-Yvon JY24) was used for Eu(III) content determination after sampling of the melt.

2.1. Analytical set-up

For investigations concerning the electrochemical behaviour of the fluoride species used for the subsequent extractions, the following electrochemical cell was used.

Mo (1 mm diameter wire), Cu (1.2 mm diameter wire) or W (1 mm diameter wire) were used as working electrodes; the auxiliary electrode was a vitreous carbon rod (3 mm diameter) with a large surface area; potentials were referred to a platinum wire (0.5 mm diameter) immersed in the molten electrolyte, acting as the quasi-reference electrode $Pt/PtO_x/O^{2-}$ [10].

2.2. Extraction set-up

Compared with the previous set-up, the extraction device needed specific arrangements. Long-term experiments cause on the one hand significant changes in the electrolyte composition and on the other hand release unacceptable gases at the graphite anode (anode effect):

- (i) as demonstrated in previous work [11], due to the change of oxide ions concentration in the bath, the platinum quasi-reference electrode was unreliable for the potential measurement. Consequently, a reference electrode separated from the electrolytic bath was used: it was a 1-mm diameter nickel wire immersed in a mixture of $LiF-CaF_2$ containing 1%

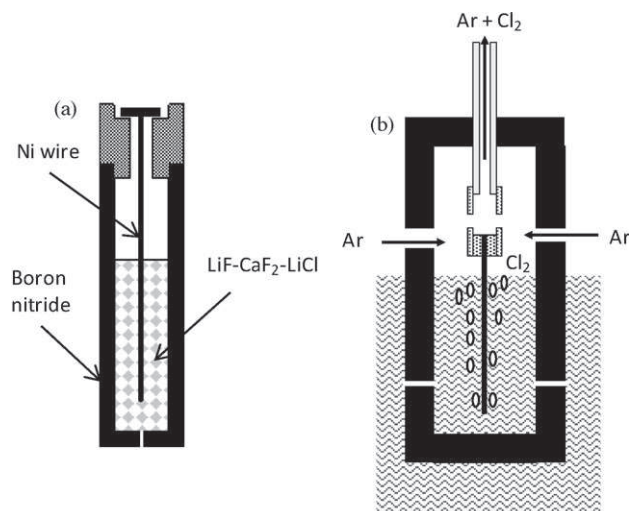


Fig. 1. Scheme of the NiF_2/Ni reference electrode scheme of the anodic compartment.

mass of NiF_2 , placed in a boron nitride cylindrical container. This reference electrode, showed in Fig. 1a, was proved to be reliable in molten fluoride baths [12] and its potential was found stable and not influenced by the change of composition of the electrolyte;

- (ii) as showed in Fig. 1b, the vitreous carbon anode was placed in a graphite compartment containing a mixture of $LiF-CaF_2-LiCl$ (10% mass). The anodic reaction was chlorine evolution instead of CF_x formation; besides, electrode compartmentalisation avoided gas to be released in the cell atmosphere and the possibility of reoxidation of Ln–M compounds formed at the cathode.
- (iii) the working electrodes were copper plates (4 cm²) and a tungsten plate (2 cm²).

2.3. Extraction experimental procedure

The extraction experimental procedure and the residual lanthanide ions concentration titration have been detailed in a previous paper [11], but are also described above:

Two kinds of working electrodes were introduced in the electrolyte:

- (iv) cathode for extraction (CE): it is a plate with a large surface area ($S_{el} = 4$ cm²). Note that the kinetics vary linearly with the ratio S_{el}/V_{sol} and thus all the following results can be extrapolated to a larger scale;
- (v) working electrode for titration of remaining Ln in the bath (TWE) which was a Cu or Ni wire immersed in the bath.

Electrolyses were performed in potentiostatic mode and the experimental procedure was the following:

- (i) recording a SW voltammogram on a TWE to determine the electrolysis potential; we took the potential of the alloying reduction peak corresponding to the formation of Cu–Eu and Al–Eu alloys.
- (ii) introduction of a EC into the bath for an electrolysis time of around 3 h to recover the alloy; this electrode was then removed from the experimental medium.
- (iii) recording a SW voltammogram on a TWE to measure the level of Ln ions remaining in the bath and, accordingly, the progress of the extraction process.

(iv) these three stages were repeated as long as any electrochemical signal was detected by SW voltammetry.

A normalized time t^* as been defined in the study of Ref. [11] and is applied in the present work:

$$t^* = t \left(\frac{S_{el}}{V_{sol}} \right) \quad (3)$$

where t is the time (h), S_{el} is the cathode surface area (cm^2), V_{sol} is the volume of the solution (cm^3) and t^* is the normalized time (h cm^{-1}).

In consequence, all the results of extraction rates can be extrapolated.

3. Results and discussion

In order to overcome the fact that the reduction of Eu(II) into Eu metal occurs at more cathodic potentials than the solvent reduction (which hinders the removal of europium from the molten salt), the activity of the electrodeposited metal must be lowered. In the present work, two different methods were attempted to decrease the metal activity: (i) the electroreduction of europium ions on a cathodic reactive substrate to form Eu-substrate alloys and (ii) the co-reduction of europium ions with another metallic ion Al(III), to directly obtain Al–Eu alloys on an inert cathode.

3.1. Europium electrochemical extraction on a reactive cathode

The first methodology, using a reactive cathode, was successfully applied in our laboratory for lanthanides extraction [7,11] and alloys preparation [13]. When a metallic cathode M reacts with an electrodeposited metal N to form an intermetallic compound MN_x , the equilibrium potential is shifted toward the positive direction; the depolarisation term is expressing the difference of standard potentials of respectively the metal N and the alloy MN_x in the molten fluoride then equal to the emf of the cell:

$$\frac{MN_x}{\text{solvent}}, \frac{N \text{ ions}}{N} \quad (4)$$

Copper seems to be an advantageous reactive cathodic material since it was shown in previous works that this element reacts easily with rare earth with a rapid kinetics at moderate temperatures (i.e. about 800–900 °C) [7].

According to the Cu–Eu phase diagram of Fig. 2 [14], europium can form four intermetallic compounds with copper. Cu_5Eu

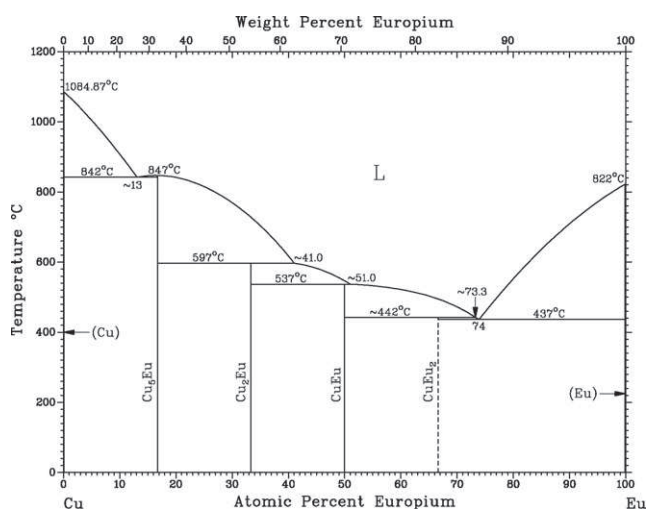


Fig. 2. Cu–Eu binary alloys phase diagram [13].

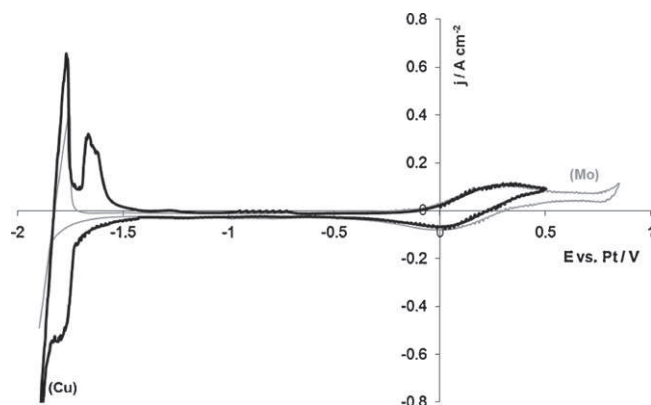


Fig. 3. Comparison of the cyclic voltammograms of the $\text{LiF–CaF}_2\text{–EuF}_3$ ($0.051 \text{ mol kg}^{-1}$) system at 100 mV s^{-1} and $T=840^\circ\text{C}$ on Mo ($S=0.315 \text{ cm}^2$) and Cu ($S=0.377 \text{ cm}^2$) electrodes. Auxiliary EL.: vitreous carbon; reference EL.: Pt.

($T_f=847^\circ\text{C}$) is the only one solid compound within the temperature range, i.e. 800–900 °C. For a temperature higher than 850 °C, all the intermetallic compounds are liquids.

Notice that the formation of liquid compounds enhances sensibly the extraction kinetics as examined in a previous paper [11].

3.1.1. Cyclic and square wave voltammetries

Fig. 3 compares the cyclic voltammograms obtained at 850 °C on molybdenum and copper electrodes at 100 mV s^{-1} . The wave around $E=0 \text{ V vs. Pt}$, corresponding to the Eu(III)/Eu(II) system identified in a previous work [6], is observed on each substrate, confirming that the reduction of Eu(III) into Eu(II) is not affected by the nature of cathodic substrate. Then, at -1.7 V vs. Pt , close to the solvent limit, a significant reduction wave is observed only on the copper cathode, with an associated anodic peak in the reverse scan. This additional peak is attributed to the formation of copper–europium alloys.

The current measured in this reduction wave can be associated to the following reaction:



where x can take the values reported on by the binary phase diagram (i.e. $x=0.5, 1, 2$ or 5).

The behaviour of Eu(III) on copper electrode was confirmed by square wave voltammetry: the comparison of square wave voltammograms carried out on Mo and Cu electrodes at 840 °C at 9 Hz is presented in Fig. 4. It can be observed first that the wave corre-

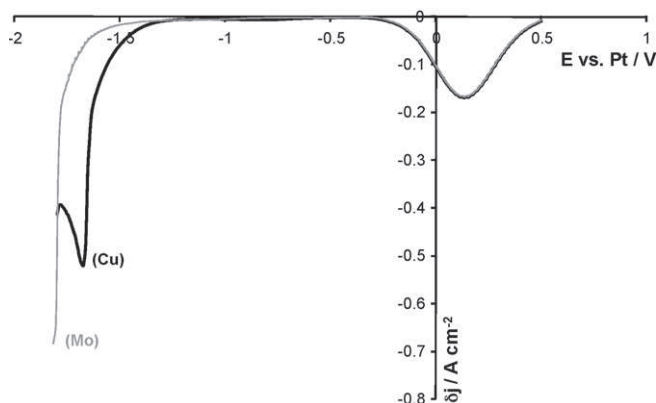


Fig. 4. Comparison of the square wave voltammograms of the $\text{LiF–CaF}_2\text{–EuF}_3$ ($0.051 \text{ mol kg}^{-1}$) system at 9 Hz and $T=840^\circ\text{C}$ on Mo ($S=0.315 \text{ cm}^2$) and Cu ($S=0.377 \text{ cm}^2$) electrodes. Auxiliary EL.: vitreous carbon; reference EL.: Pt.

sponding to the Eu(III)/Eu(II) system is identical on both substrates whereas on Cu electrode, and then a new reduction peak, corresponding to the Cu–Eu alloys formation.

3.1.2. Observation and characterisation of the Eu–Cu alloys

In order to characterise the obtained intermetallic compounds, the electrodeposition of europium–copper alloys was performed by cathodic polarization of a copper plate at -200 mA cm^{-2} at 850°C during 1 h. The cross section of the plate obtained after the electrolysis run was observed by scanning electron microscopy. An EDS probe allowed determining the composition of each phase present on the micrograph.

Two different compounds were identified on the micrographs presented in Fig. 5a and b:

- (i) the first one was a homogeneous Cu_5Eu coating located in the external part of the electrode. The thickness of the layer for a relatively short electrolysis time suggests that the intermetallic diffusion process Eu/Cu is quite fast at 850°C ;
- (ii) on the magnification on the previous observation (Fig. 5b), metallic particles containing CuEu_2 and little amount of Eu are visible in the frozen salt stuck on the electrode. It is assumed that these compounds were produced during the cooling of the sample. Indeed, according to the Cu–Eu phase diagram, the cooling step of the liquid alloy yields in its segregation in CuEu_2 and Eu. According to previous results, even if europium metal is not stable since it reacts with lithium ion, the quenching of the electrode and its rapid withdrawal from the cell allows Eu metal to be observed.

These experiments showed that europium ions can be extracted from the melt using the reactive copper cathodes.

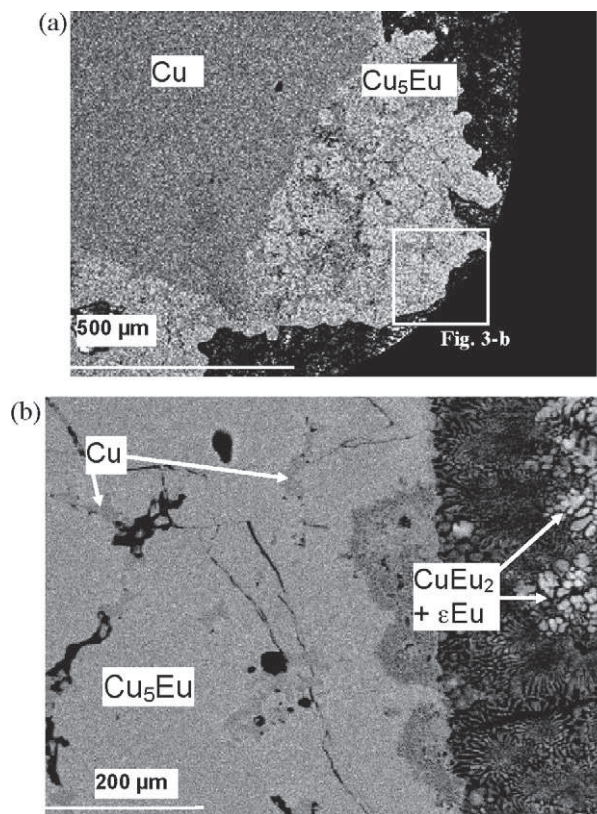


Fig. 5. (a and b) SEM micrographs of the cross section of copper plate after galvanostatic electrolysis at -200 mA cm^{-2} during 1 h and $T=840^\circ\text{C}$.

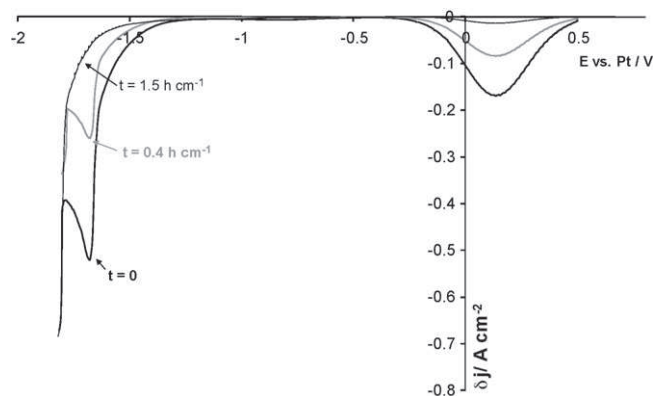


Fig. 6. Variation of the square wave voltammograms of the $\text{LiF–CaF}_2\text{–EuF}_3$ system at 100 mV s^{-1} and $T=840^\circ\text{C}$ for several electrolysis times. Working EL.: Cu; auxiliary EL.: vitreous carbon; reference EL.: Pt.

3.1.3. Evaluation of extraction efficiency on Cu electrode

The measurement of the potential difference between the Eu–Cu alloys formation and the solvent reduction allows the europium theoretical extraction efficiency to be estimated. This relationship, using the Nernst law, as already been presented in other works [15]:

$$\eta = 1 - \exp\left(\frac{-nF}{RT} \Delta E\right) \quad (6)$$

where η is the extraction efficiency, n the number of exchanged electrons, T the absolute temperature and ΔE the potential difference between the respective Eu(II) and solvent reductions.

The measurement of ΔE on the cyclic voltammogram of Fig. 3 yields a value around 116 mV.

Consequently, with $T=850^\circ\text{C}$ and $n=2$, the theoretical extraction efficiency for europium on copper is estimated to be 91%.

3.1.4. Electrochemical extraction

Extraction experiments were performed on a Cu cathode at $T=850^\circ\text{C}$ in potentiostatic mode, using a potential of -1.7 V vs. Pt , which corresponds to the peak of Eu–Cu alloys formation.

Typical SW voltammograms plotted on Cu at different extraction durations (0, 0.4 and 1.5 h cm^{-1}) are presented in Fig. 6. One can observe on these voltammograms a significant decrease of the current density with the electrolysis duration, correlated to the decrease of Eu(III) content. Furthermore, the current density decreases more rapidly at the beginning of the experiment than after longer times. Using the calibration curves previously obtained, the measurement of the cathodic peak current density allowed the residual Eu(III) concentration in the melt, and thus the extraction efficiency to be determined.

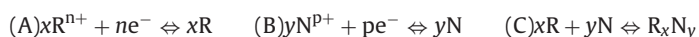
The extraction efficiency progress vs. the normalized time is presented in Fig. 7: the maximum extraction efficiency is obtained after 1.4 h cm^{-1} . We can notice that it is sensibly less than 1, as predicted above. The bath was sampled at the end of the experiments, and according to the ICP–AES titration, the final extraction efficiency was determined to be 92%. This result is in excellent agreement with the theoretical extraction efficiency estimated using cyclic voltammetry measurement (91%).

The Eu(III) extraction has been realised on a copper reactive cathode and a good extraction efficiency was achieved by forming Eu–Cu alloys. However, for the purpose of nuclear applications, a more efficient extraction of europium ions might be required in order to recycle the solvent. Consequently, the other technique of electrochemical co-reduction between europium and aluminium ions must be attempted if we aim to obtain higher extraction efficiencies.

3.2. Europium electrochemical extraction by co-reduction with aluminium ions

The simultaneous reduction of two metallic ions on an inert electrode resulting in an alloy of the two metals is based on the same principle as the reactive cathode: a decrease of the activity of the electrodeposited lanthanide metal is obtained by addition of aluminium ions [16]. This process was early proposed by Taxil et al. in molten salts for nuclear wastes reprocessing [17].

If R is the most reactive metal, N the less reactive one and R_xN_y the alloy formed by co-reduction, the co-reduction process of two metallic ions R^{n+} and N^{p+} involves the following reactions:



The overall process is : $xR^{n+} + yN^{p+} + (n+p)e^- \rightleftharpoons R_xN_y$ (7)

The equilibrium potential of the system R/R_xN_y can be expressed as:

$$E_{R^{n+}/R_xN_y} = E_{R^{n+}/R} - \frac{RT}{nF} \ln [a_R(\text{in } R_xN_y)] \quad (8)$$

where $E_{R^{n+}/R}$ is the equilibrium potential of pure R element and $a_R(\text{in } R_xN_y)$ the activity of R in the intermetallic compound R_xN_y .

As a_R in R_xN_y is less than one, it can be deduced that $E_{R^{n+}/R_xN_y} > E_{R^{n+}/R}$. As a consequence, the co-deposition of R with a more noble metal allows R^{n+} to be reduced at a potential more anodic than the pure metal deposition: this is the "depolarisation effect". Moreover, this technique is selective since the alloy composition depends on the imposed potential [18].

3.2.1. Electrochemical behaviour of europium-aluminium system

The Al-Eu phase diagram [14] mentions 3 intermetallic compounds (Al_4Eu , Al_2Eu and $AlEu$) which could be obtained by co-reduction between aluminium and europium ions.

A previous study in our laboratory of the Al(III) electrochemical behaviour has shown that the reduction of Al(III) in Al proceeds in a one step exchanging 3 electrons [19]. On the cyclic voltammogram presented in Fig. 8, the wave observed at -1.25 V vs. Pt is attributed to:



On the square wave voltammogram plotted at 9 Hz in Fig. 7, a reduction peak at -1.1 V vs. Pt is also observed; it corresponds to the aluminium deposition.

Figs. 8 and 9 compare the cyclic voltammograms and square wave voltammograms of AlF_3 (grey thin lines), EuF_3 (grey thick lines) and a mixture of AlF_3 - EuF_3 (black lines) in molten LiF - CaF_2 at $860^\circ C$, respectively.

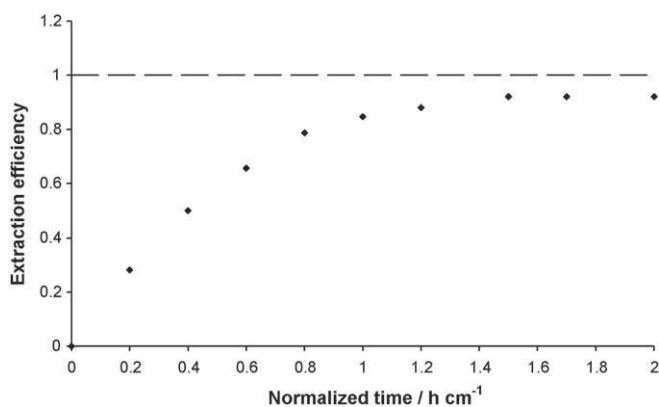


Fig. 7. Variation of the europium extraction efficiency at $T=840^\circ C$ vs. time. Working El.: Cu; auxiliary El.: vitreous carbon; reference El.: Pt.

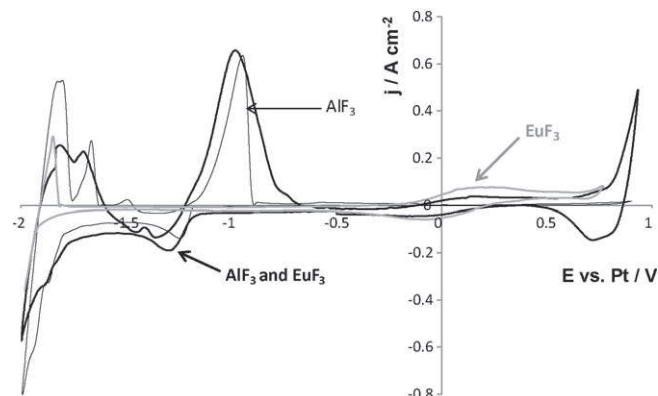


Fig. 8. Comparison of the cyclic voltammograms of the LiF - CaF_2 - $EuF_3(0.013 \text{ mol kg}^{-1})$ - $AlF_3(0.052 \text{ mol kg}^{-1})$ system at 100 mV s^{-1} and $T=840^\circ C$ on W ($S=0.315 \text{ cm}^2$) electrode. Auxiliary El.: vitreous carbon; reference El.: Pt.

- The previous results on the reduction of Al(III) are confirmed: reduction peak Al(III)/Al at -1.25 V vs. Pt and reoxidation peak at -1.2 V vs. Pt.
- The simultaneous reduction of aluminium and europium ions produces a noticeable change in the electrochemical signal on both voltammograms attributed to Al-Eu formation.
 - Increase of the peak current density of the Al(III)/Al system with a shift in the negative sense.
 - Shoulders for $E < -1.25$ V vs. Pt (pure aluminium deposition): -1.46 , -1.67 and -1.74 V vs. Pt.

We can notice once again that the Eu(III)/Eu(II) reduction wave at about 0 V vs. Pt is unchanged in presence of Al(III).

3.2.2. Co-reduction products analysis

To characterise the Al-Eu alloys formation at several potentials, potentiostatic electrolyses were performed at $T=840^\circ C$ during 1200 s. The electrode was quenched after each run and the deposited product was cleaned, polished and analysed by an EDS probe. The applied electrolysis potentials were evaluated from the square wave voltammogram (Fig. 9) and results are described separately for the following two potential regions:

- $E > -1$ V vs. Pt
 - At these potentials, only the electrochemical reduction of Eu(III) into Eu(II) occurs. None of the electrolyses led to Al-Eu

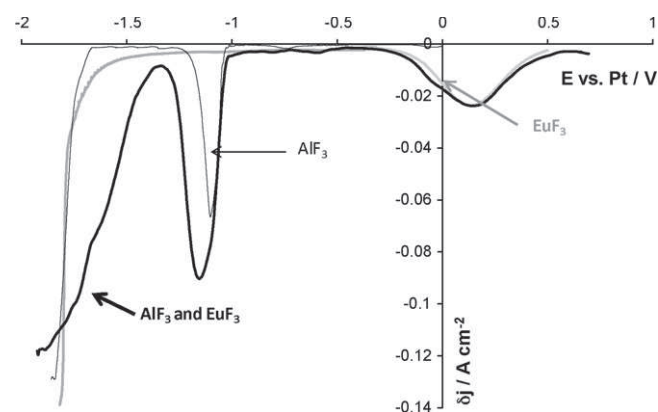


Fig. 9. Comparison of the square wave voltammograms of the LiF - CaF_2 - $EuF_3(0.013 \text{ mol kg}^{-1})$ - $AlF_3(0.052 \text{ mol kg}^{-1})$ system at 9 Hz and $T=840^\circ C$ on W ($S=0.315 \text{ cm}^2$) electrode. Auxiliary El.: vitreous carbon; reference El.: Pt.

alloy deposition. This observation is in agreement with the co-reduction theory [8,16] where only the metallic deposition Eu(II)/Eu wave can be depolarised. Therefore, the Eu(III)/Eu(II) wave is not influenced by the presence of aluminium ions in the molten solvent.

- $E < -1$ V vs. Pt

All the electrolyses performed at a potential lower than -1 V vs. Pt (at -1.1 , -1.25 , -1.5 and -1.6 V vs. Pt) yield a unique compound Al_4Eu as shown in Fig. 10. This figure highlights that the reduction of Eu(II) is sensibly depolarised in presence of aluminium ions and the co-reduction process can be written as:



The Al–Eu alloys are formed at the cathode surface, then released in the salt in the form of micro-particles ($10 \mu\text{m}$ diameter), having a uniform composition Al_4Eu .

3.2.3. Electrochemical extraction

The europium extraction was realised on tungsten plate in LiF-CaF_2 media at $T = 840^\circ\text{C}$.

Potenstostatic electrolyses were carried out and *in situ* measurements of the Eu content were realised using square wave voltammetry. According to Eq. (5), on the base of 2 exchanged electrons (Eu(II)/Eu), a complete extraction of europium should be achieved using a minimum difference $\Delta E = -0.44$ V vs. solvent. As a consequence, the electrolysis potential was chosen equal to -1.2 V vs. Pt or -0.6 V/solvent.

The tungsten electrode was replaced every 3 h and the progress of the reaction was periodically followed by cyclic and square wave voltammograms on a tungsten wire. Typical square wave voltammograms are presented in Fig. 11 where a significant decrease of the current density is observed, correlated to the decrease of Al(III) and Eu(III) ions concentration in the bath during the extraction process. As showed in Fig. 12, the concentration decreased more quickly at the beginning of the electrolysis.

Electrolyses were performed during 3.5 h cm^{-1} to obtain a cathodic current density value approaching zero on the square wave voltammogram. The extraction efficiency was calculated with ICP analysis of the salt after 3.5 h cm^{-1} electrolysis and was equal to 99.6% for Eu(III) .

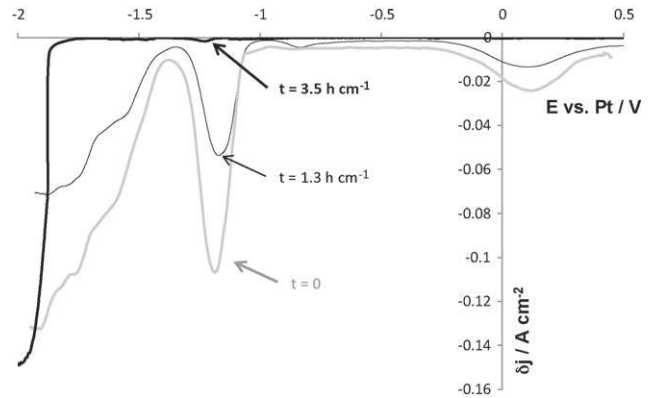


Fig. 11. Variation of the square wave voltammograms of the $\text{LiF-CaF}_2\text{-EuF}_3\text{-AlF}_3$ system at 100 mV s^{-1} and $T = 840^\circ\text{C}$ for several electrolysis times on W. Auxiliary EL.: vitreous carbon; reference EL.: Pt.

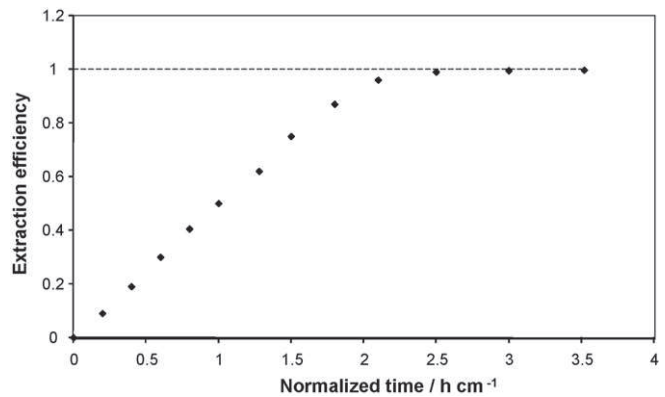


Fig. 12. Variation of the europium extraction efficiency at $T = 840^\circ\text{C}$ vs. normalized time.

4. Conclusions

In the frame of the cleaning of fluoride salts utilized for nuclear applications (which is required either after spent fuel partitioning by pyrochemical methods or during the MSR salt treatment), the removal of Eu(III) ions from a molten fluoride solvent (LiF-CaF_2) has been performed by electrodeposition in the form of intermetallic compounds. Two electrochemical methods (taking place after a complete removal of actinides, which would be deposited prior Eu), yielding different results on the final efficiency, were carried out:

Reduction on reactive electrode (copper), yielding an extraction efficiency of 91% in 2 h cm^{-1} . This relatively short duration makes this methodology convenient for an extraction process if about 10% of initial Eu(III) content could be left in the solution.

Co-reduction with aluminium ions, yielding a complete extraction ($\eta > 99.6\%$ in 3 h cm^{-1}) but needing longer extraction duration and the addition of Al(III) ions in the solution. Depending on the future use of the salt, the excess Al(III) ions could then be removed by liquid Al electrodeposition (on a carbon cathode for instance) or left in the solvent.

Acknowledgments

The authors express their thanks to the French CNRS PACEN program (GDR PARIS and PCR ANSF) for financial support of this work.

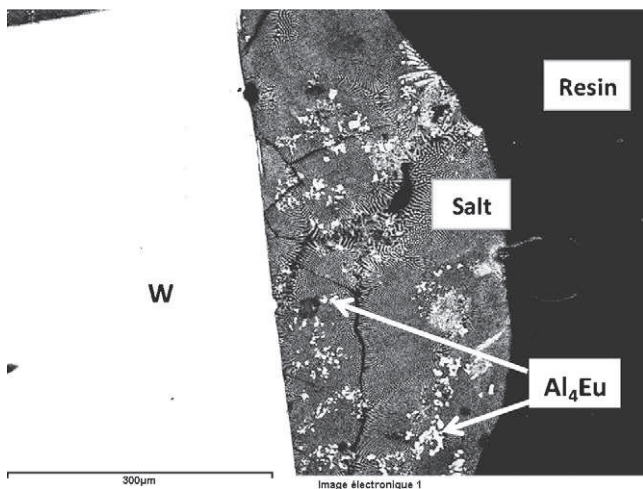


Fig. 10. SEM micrographs of the cross section of tungsten plate after potentiostatic electrolysis at -1.1 V vs. Pt during 1200 s and $T = 840^\circ\text{C}$.

References

- [1] J.P. Schapira, Nucl. Phys. A 654 (1999) C458.
- [2] O. Conocar, N. Douyere, J.P. Glatz, J. Lacquement, R. Malmbeck, J. Serp, Nucl. Sci. Eng. 153 (2006) 253.
- [3] J. Serp, M. Allibert, A. Le Terrier, R. Malmbeck, M. Ougier, J. Rebizant, J.P. Glatz, J. Electrochem. Soc. 152 (2005) C167.
- [4] S. Delpech, E. Merle-Lucotte, D. Heuer, M. Allibert, V. Ghetta, C. Le Brun, X. Doligez, G. Picard, J. Fluorine Chem. 130 (2009) 11.
- [5] P. Taxil, L. Massot, C. Nourry, M. Gibilaro, P. Chamelot, L. Cassayre, J. Fluorine Chem. 130 (2009) 94.
- [6] L. Massot, P. Chamelot, L. Cassayre, P. Taxil, Electrochim Acta 54 (2009) 6361.
- [7] C. Nourry, L. Massot, P. Chamelot, P. Taxil, J. Appl. Electrochem. 39 (2009) 927.
- [8] M. Gibilaro, L. Massot, P. Chamelot, P. Taxil, J. Nucl. Mater. 382 (2008) 39.
- [9] P. Chamelot, P. Taxil, B. Lafage, Electrochim. Acta 39 (1994) 2571.
- [10] Y. Berghoute, A. Salmi, F. Lantelme, J. Electroanal. Chem. 365 (1994) 171.
- [11] C. Nourry, L. Massot, P. Chamelot, P. Taxil, J. Appl. Electrochem., in press, doi:10.1007/s10800-009-9922-2.
- [12] P. Taxil, Z. Qiao, J. Chim. Phys. 82 (1985) 83.
- [13] C. Nourry, L. Massot, P. Chamelot, P. Taxil, J. New Mater. Electrochem. Syst. 10 (2007) 117.
- [14] ASM International, Binary Alloy Phase Diagrams, 2nd ed., ASM International, Materials Park, 1996.
- [15] P. Chamelot, L. Massot, C. Hamel, C. Nourry, P. Taxil, J. Nucl. Mater. 360 (2007) 64.
- [16] A. Brenner, Electrodeposition of Alloys, vol. 1, Academic Press, New York, 1963.
- [17] P. Taxil, P. Chamelot, L. Massot, C. Hamel, J. Miner. Met. 39 (2003) 177.
- [18] M. Gibilaro, L. Massot, P. Chamelot, P. Taxil, Electrochim. Acta 54 (2009) 5300.
- [19] M. Gibilaro, L. Massot, P. Chamelot, P. Taxil, J. Alloy Compds. 471 (2009) 412.